# Optimization of green synthesis of silver nanoparticles using Response Surface Method (RSM)

IOP Conf. Series: Materials Science and Engineering **805** (2020) 012022 doi:10.1088/1757-899X/805/1/012022

# Optimization of green synthesis of silver nanoparticles using Response Surface Method (RSM)

M Ibrahim[*1], JB Agboola[2], AS Abdulkareem[3,5], O Adedipe[1] and JO Tijani[4,5]

[1]Department of Mechanical Engineering, Federal University of Technology, Minna.

[2]Materials and Metallurgical Engineering Department, Federal University of Technology, Minna.

[3,]Department of Chemical Engineering, Federal University of Technology, Minna.

[4]Department of chemistry, Federal University of Technology, Minna.

[5]Nanotechnology Research Group, Centre for Biotechnology and Genetic Engineering, Federal University of Technology, Minna.

*Corresponding author: Ibrahim M. (abuhannatu@yahoo.com).

## Abstract

This study is aimed at investigating the effect of synthesis parameters such as temperature, pH, volume of precursor and volume of extract on the crystal size of silver nanoparticles (AgNPs) synthesized via plant extract of *Piptadeniastrum africanum* (African Oak) using $2^4$ factorial experimental design. The synthesized nanoparticles were characterized by X-ray Diffraction (XRD) and High Resolution Scanning Electron Spectroscopy (HRSEM) fitted with Energy Dispersive Spectroscopy (EDS). The optimum values of the synthesis parameters were found to be: pH 8, reaction temperature 35 $^{o}$C, the ratio of the volume of extract to the volume of precursor was kept at 1:10 while silver nitrate $(AgNO_3)_{aq}$ solution was maintained at 1 mM concentration. The HRSEM and XRD analysis showed that the morphology of the nanoparticles is spherical with an average crystal size of 20-25 nm.

**Keywords**: Synthesis parameters, crystallite size, silver nanoparticles, green synthesis, factorial experimental design, characterization

## 1 Introduction

Metallic nanoparticles have recently attracted attentions due to their unique physicochemical properties. These special properties and especially the size give them an edge over other materials. This improves their applications in various human activities [1]. Nanoparticles synthesis basically consist of reduction of metal salt in its oxidation state to zero-valence state called nanoparticles. Nanoparticles can be synthesized using physical methods, chemical methods, and biological methods. The physical and chemical methods of synthesis are complicated because they are carried out using separate stabilizing and capping agents; they are also expensive and they are hazardous to human health due to toxic fumes that are radiated from the chemicals involved. Recently, green synthesis method is preferably used for the synthesis of metallic nanoparticles. Plants and plant extracts play dual role as a reducing, capping and stabilizing agents. In addition, the method is a one pot procedure, economical and more environmentally friendly.

Silver nanoparticles (AgNPs) have wide applications in medical field, water purification, improvement in mechanical properties and corrosion protection of some engineering materials. The green synthesis method is governed by several factors such as temperature, pH, reaction time, volume of metal salt and volume of plant extract. The interaction of these synthesis factors plays a vital role in determining shape and size of synthesized Ag-NPs. Despite numerous studies carried out on synthesis of AgNPs, experimental optimization of operational parameters and factors influencing the crystal size of AgNPs has not been given adequate consideration. Therefore, this study investigates the optimization of the synthesis parameters of AgNPs using Response Surface Method (RSM).

## 2 Materials and Methods

### 2.1 Materials

Chemicals used in the study include silver nitrate ($AgNO_3$) purchased from Sigma Aldrich, concentrated hydrochloric acid (HCl) and sodium hydroxide (NaOH) purchased from Kermel England and distilled water. All the chemicals used have percentage purity in the range of 95-99%. Some of the equipment used in the study includes digital weighing balance, pH meter,

magnetic stirrer and hot plate, uv-spectrometer, high resolution scanning electron microscopy, X-ray diffractometer, freeze drying machine and high speed refrigerated centrifuge.

## 2.2 Methodology

### 2.2.1 Collection and preparation of plant material

Fresh leaves of *Piptadeniastrum africanum* were collected at Bosso area in Minna, Niger State Nigeria. The leaves were thoroughly washed with running tap water and distilled water in order to remove dust and other contaminants and then dried under shade for seven days. The dried leaves were pounded into homogeneous powder using mortar and pestle. The obtained powder was then kept under dry condition for future use.

### 2.2.2 Preparation of aqueous leaf extracts of *Piptadeniastrum africanum*

Ten grams (10 g) of powdered leaf of *P. africanum* was mixed with 100 ml of distilled water in a 250 ml beaker and the mixture was boiled at 60 $^{o}$C for 15 min using magnetic hot plate and stirrer. The extract was obtained by filtration using Whatman no.1 filter paper and stored in brown bottle under room temperature for future use.

### 2.2.3 Phytochemical analysis of *Piptadeniastrum africanum* leaf

The phytochemical analysis of *Piptadeniastrum africana* leaf extract was carried out in accordance with AOAC methods and reported by Singleton *et al.* [2].

### 2.2.4 Synthesis of silver nanoparticles using aqueous leaf extracts of *P. africanum* and experimental optimization of synthesis parameters

Silver nanoparticles were synthesized by the mixture of 1 ml of aqueous solution of *P. africanum* leaf extract to 10 ml of 1 mM $AgNO_3$ in a 250 ml beaker while the pH was adjusted to a value of 8 using few drops of 2 M solution of NaOH. The reaction was allowed to take place at room temperature for 60 min. The crystal size of the formed AgNPs was calculated using Derby-Scherrer's equation [3].

$$D = \frac{K\lambda}{\beta Cos\Phi} \qquad (1)$$

Where Φ is the peak width angle, $K$ is the shape factor = 0.89, β is the full width at half maximum of the XRD peak, and λ is the wavelength of light used for diffraction = 1.541Å.

In order to determine the optimum crystal size, four synthesis parameters; reaction temperature, pH, volume of extract and volume of silver nitrate ($AgNO_3$) aqueous solution were varied and the optimization procedure was carried out using $2^4$ factorial design of experiment (DOE). Many authors have reported the synthesis of silver nanoparticles within certain range of synthesis conditions. However, the two level factors chosen for this work were based on previous studies and were considered only after preliminary investigations. low level (-) indicate variable values that were considered as low limits and high level (+) indicate variable values that were considered as upper limit as shown in Table 1.

**Table 1**. High and Low values for $2^4$ Factorial Design the for synthesis of AgNPs

| Variables | Reaction Temp ($^oC$) | pH | $AgNO_3$ vol. (ml) | Extract vol. (ml) |
|---|---|---|---|---|
| L/ L | 35.00 | 8.00 | 10.00 | 1.00 |
| H/L | 60.00 | 9.00 | 50.00 | 3.00 |

Design Expert software was used to carry out statistical Analysis of Variance (ANOVA), so that the main as well as the combined effects of the parameters considered are represented in empirical models to show the effect of these parameters on the crystal size.

### 2.2.5 Characterization of Ag-NPs

The synthesized nanoparticles were characterized by X-ray Diffraction (XRD) and High Resolution Scanning Electron Spectroscopy (HRSEM) fitted with Energy Dispersive Spectroscopy (EDS).

## 3 Results and Discussion

### 3.1 Phytochemical analysis of *Piptadeniastrum africanum* leaf extract

The result of phytochemical analysis on *P. africanum* leaf extract shows the presence of some prominent biomolecules such as phenols, flavonoids and tannins as presented in Table 2 which are the active ingredients in the plant.

**Table 2**. Phytochemical attributes of *P. africanum* leaf extract

| S/N | Phytochemicals | Result |
|---|---|---|
| 1. | Phenol | + |
| 2. | Flavonoids | + |
| 3. | Tannins | + |

### 3.2 Experimental optimization of the synthesis

All the sixteen samples obtained from $2^4$ factorial design of experiment were synthesized and characterized by X-ray diffraction (XRD) analysis and the crystal size was calculated by Derby Scherrer's equation. Table 3 shows $2^4$ factorial design of experiment with the corresponding responses (crystal size).

**Table 3**. Experimental matrix for $2^4$ factorial design for the synthesis of AgNPs

| Run | R.Temp. $^oC$ | pH | P/cursor vol. (ml) | Ext.vol. (ml) | Crsyt. Size (nm) |
|---|---|---|---|---|---|
| 1 | 35.00 | 9.00 | 50.00 | 1.00 | 20.2 |
| 2 | 35.00 | 9.00 | 10.00 | 3.00 | 18.4 |
| 3 | 35.00 | 9.00 | 50.00 | 3.00 | 22.5 |
| 4 | 60.00 | 9.00 | 50.00 | 1.00 | 25.0 |
| 5 | 60.00 | 8.00 | 50.00 | 1.00 | 25.5 |
| 6 | 60.00 | 9.00 | 10.00 | 3.00 | 25.8 |
| 7 | 35.00 | 8.00 | 10.00 | 1.00 | 28.0 |
| 8 | 35.00 | 8.00 | 50.00 | 3.00 | 28.7 |
| 9 | 60.00 | 9.00 | 10.00 | 1.00 | 30.0 |
| 10 | 60.00 | 9.00 | 50.00 | 3.00 | 30.2 |
| 11 | 60.00 | 8.00 | 10.00 | 3.00 | 30.5 |
| 12 | 35.00 | 8.00 | 50.00 | 1.00 | 34.4 |
| 13 | 60.00 | 8.00 | 50.00 | 3.00 | 42.6 |
| 14 | 35.00 | 9.00 | 10.00 | 1.00 | 25.9 |
| 15 | 60.00 | 8.00 | 10.00 | 1.00 | 20.6 |
| 16 | 35.00 | 8.00 | 10.00 | 1.00 | 15.4 |

### 3.3 Numerical Optimization

#### 3.3.1 Evaluation

The model terms are temperature (A), pH (B), volume of precursor (C) and extract volume (D). Three factor interaction (3FI) model was utilized and no aliases were found in the model. The degrees of freedom for the model, residuals, lack of fit and pure error are 14, 1, 1 and 0 respectively while the average leverage of the model is 0.9375. The model F-value of 19.55 in Table 4 shows that the model is significant. The model terms (A, B, C, D) are also shown to be significant based on "prob>F" < 0.05. The ANOVA analysis also show that Std. Dev. = 2.05, R-Squared = 0.9572, Mean = 25.63, Adj R-Squared = 0.9082, C.V. % = 8.00, Pred R-Squared = 0.7762, PRESS = 153.59, Adeq Precision = 14.200.

The predicted R-squared value of 0.7762 is in reasonable agreement with the Adjusted R-squared value of 0.9082, while the adequate precision value of 14.200 indicated an adequate signal.

The final regression equations generated in terms of coded factor is given by:

Crystallite size = 25.63 +2.69A + 3.75B + 2.84C + 2.85D + 1.01BC - 0.95BD + 0.44CD - 1.21BCD…….(2)

while the final regression equation in terms of actual factor is given by:

Cystallite size = 15.06 + 0.22 temp. - 0.98 pH - 45.95Ext. Vol.- 1.16Salt Vol.+ 5.66 pH * Ext.vol. + 0.15 pH * salt vol. + 1.05 * Ext. vol * salt vol. - 0.12 * pH * Ext.vol. * salt vol……(3)

**Table 4**. ANOVA for the factorial model

| Source | Sum of Square | Df | Mean Square | F-value | P-value Prob>F | Remark |
|---|---|---|---|---|---|---|
| Model | 656.77 | 8 | 82.10 | 19.55 | 0.0004 | Significant |
| A-Tempt. | 115.56 | 1 | 115.56 | 27.52 | 0.0012 | |
| B-pH | 225.00 | 1 | 225.00 | 53.38 | 0.0002 | |
| C-Ext. vol. | 128.00 | 1 | 128.00 | 30.67 | 0.0009 | |
| D-Salt vol. | 129.96 | 1 | 129.96 | 30.75 | 0.0008 | |
| BC | 16.40 | 1 | 16.40 | 3.91 | 0.0887 | |
| BD | 14.44 | 1 | 14.44 | 3.44 | 0.1061 | |
| CD | 3.06 | 1 | 3.06 | 0.73 | 0.4214 | |
| BCD | 23. 52 | 1 | 23.52 | 5.63 | 0.0499 | |
| Residual | 29.40 | 7 | 4.20 | | | |
| Corr.Total | 686.17 | 15 | | | | |

### 3.3.2 Diagnostic Plots

The diagnostic plots are shown in Figure 1, while the overall diagnostic case statistics is presented in Table 5. It can be seen that the actual values and the predicted values of are in close agreement.

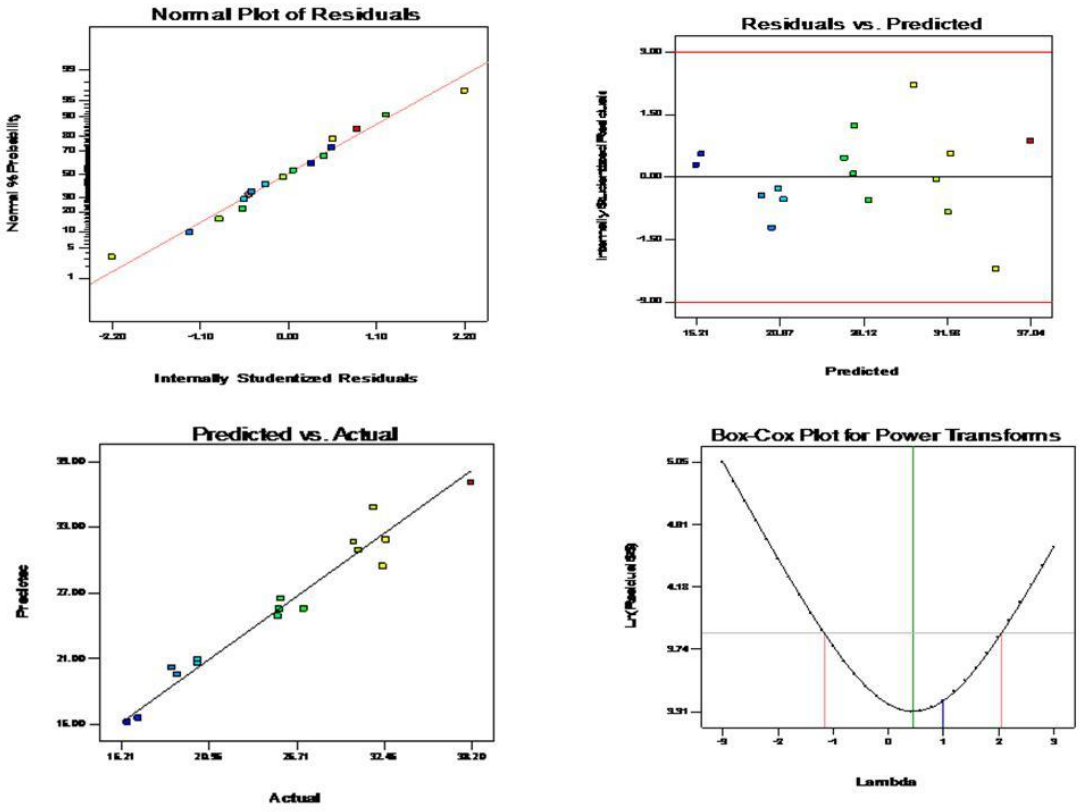


**Figure 1**. The diagnostic plots of the responses

**Table 5**. Diagnostic case statistics

| Stand Order | Actl Val. | Pred. Val. | Resid | Int. studt Res. | Ext studt Res. | Influence fitted val DFFIT | cooks Dist. | Run Order |
|---|---|---|---|---|---|---|---|---|
| 1 | 15.60 | 15.21 | 0.39 | 0.286 | 0.266 | 0.302 | 0.012 | 13 |
| 2 | 20.20 | 20.59 | -0.39 | -0.286 | -0.266 | -0.302 | 0.012 | 11 |
| 3 | 18.50 | 20.16 | -1.66 | -1.226 | -1.282 | -1.453 | 0.215 | 12 |
| 4 | 27.20 | 25.54 | 1.66 | 1.226 | 1.282 | 1.453 | 0.215 | 5 |
| 5 | 16.30 | 15.5 | 0.74 | 0.544 | 0.515 | 0.584 | 0.042 | 14 |
| 6 | 20.20 | 20.94 | -0.74 | -0.544 | -0.515 | -0.584 | 0.044 | 8 |
| 7 | 32.40 | 29.41 | 2.99 | 2.204 | 3.688 | 4.18 | 0.694 | 3 |
| 8 | 31.80 | 34.79 | -2.99 | -2.204 | -3.688 | -4.18 | 0.694 | 16 |
| 9 | 18.90 | 19.51 | - 0.61 | -0.452 | -0.452 | -0.481 | 0.929 | 1 |
| 10 | 25.50 | 24.89 | 0.61 | 0.452 | 0.452 | 0.481 | 0.029 | 4 |
| 11 | 25.80 | 5.51 | 0.087 | 0.065 | 0.060 | 0.068 | 0.001 | 2 |
| 12 | 30.80 | 0.89 | -0.088 | -0.065 | -0.060 | -0.06 | 0.001 | 10 |
| 13 | 25.70 | 0.46 | -0.26 | -0.563 | -0.533 | -0.604 | 0.045 | 9 |
| 14 | 32.60 | 1.84 | 0.26 | 0.563 | 0.533 | 0.604 | 0.045 | 7 |
| 15 | 30.50 | 1.66 | -1.16 | -0.858 | -0.839 | -0.952 | 0.106 | 15 |
| 16 | 38.20 | 37.04 | 1.16 | 0.858 | 0.839 | 0.9.52 | 0.105 | 6 |

The criteria set for the numerical optimization of the various synthesis factors are detailed in Table 6.

**Table 6**. Optimization constraints

| Name | Goal | Upper Limit | Lower Limit | Upper Weight | Lower Weight | Import |
|---|---|---|---|---|---|---|
| Temp. | in range | 60 | 35 | 1 | 1 | 3 |
| pH | in range | 9 | 8 | 1 | 1 | 3 |
| Ext. vol. | in range | 3 | 1 | 1 | 3 | 3 |
| Salt vol. | in range | 50 | 10 | 1 | 1 | 3 |
| Cryt. Size | Minimize | 38.2 | 15.4 | | | |

The result presented in Table 7 indicated that the least crystallite size of 15.43 nm was obtained for the synthesis condition of temperature 35 $^{o}$C, pH 8, and extract to salt volume ratio of 1:10. These conditions were used for the synthesis of AgNPs in this study.

**Table 7**. Final optimized synthesis parameters

| No. | Temp. | pH | Ext.vol. | Salt vol. | Cryt. Size | Desblty |
|---|---|---|---|---|---|---|
| 1 | 35.00 | 8.00 | 1.00 | 10.00 | 15.43 | 1.0 Selected |
| 2 | 35.16 | 8.01 | 2.15 | 10.05 | 15.55 | 1.0 |
| 3 | 35.06 | 8.02 | 2.09 | 10.02 | 15.58 | 1.0 |
| 4 | 36.30 | 8.01 | 1.21 | 10.13 | 15.58 | 1.0 |
| 5 | 35.43 | 8.00 | 1.00 | 11.67 | 15.49 | 1.0 |
| 6 | 35.98 | 8.00 | 1.01 | 10.28 | 15.46 | 1.0 |
| 7 | 35.61 | 8.01 | 1.23 | 10.19 | 15.48 | 1.0 |
| 8 | 35.07 | 8.00 | 2.46 | 10.07 | 15.35 | 1.0 |
| 9 | 35.87 | 8.01 | 1.27 | 10.10 | 15.53 | 1.0 |
| 10 | 35.50 | 8.00 | 1.26 | 10.63 | 15.46 | 1.0 |
| 11 | 35.98 | 8.00 | 1.61 | 10.09 | 15.55 | 1.0 |
| 12 | 35.00 | 8.00 | 1.01 | 13.50 | 15.60 | 1.0 |
| 13 | 35.03 | 8.00 | 2.94 | 10.02 | 15.59 | 1.0 |
| 14 | 35.06 | 8.00 | 2.15 | 10.76 | 15.59 | 1.0 |
| 15 | 35.07 | 8.00 | 2.74 | 10.05 | 15.57 | 1.0 |
| 16 | 35.69 | 8.00 | 1.66 | 10.44 | 15.56 | 1.0 |
| 17 | 36.28 | 8.01 | 1.10 | 10.43 | 15.60 | 1.0 |
| 18 | 36.03 | 8.00 | 1.33 | 10.02 | 15.52 | 1.0 |
| 19 | 35.17 | 8.00 | 2.87 | 10.01 | 15.59 | 1.0 |
| 20 | 35.42 | 8.00 | 1.21 | 10.40 | 15.40 | 1.0 |
| 21 | 35.92 | 8.01 | 1.01 | 10.26 | 15.51 | 1.0 |
| 22 | 35.01 | 8.01 | 2.11 | 10.45 | 15.59 | 1.0 |
| 23 | 37.18 | 8.00 | 1.00 | 11.02 | 15.79 | 0.992 |
| 24 | 35.08 | 8.10 | 2.83 | 10.00 | 16.83 | 0.945 |
| 25 | 35.00 | 8.00 | 1.01 | 38.78 | 18.33 | 0.879 |
| 26 | 35.00 | 8.00 | 1.01 | 44.71 | 18.96 | 0.851 |
| 27 | 51.95 | 8.03 | 1.00 | 10.00 | 19.00 | 0.849 |
| 28 | 35.00 | 8.00 | 1.00 | 45.80 | 19.08 | 0.846 |
| 29 | 35.00 | 8.01 | 3.00 | 36.33 | 22.80 | 0.682 |
| 30 | 35.09 | 8.44 | 1.84 | 50.00 | 24.93 | 0.587 |

### 3.4 Characterization of AgNPs

#### 3.4.1 UV-vis spectroscopy

Figure 2 shows UV-vis spectrum of as-synthesized AgNPs. The UV-vis spectrum shows the characteristic surface plasmon resonance band (SPR) at maximum absorption peak corresponding to the wavelength of 400 nm which is within the range previously reported for AgNPs [4].

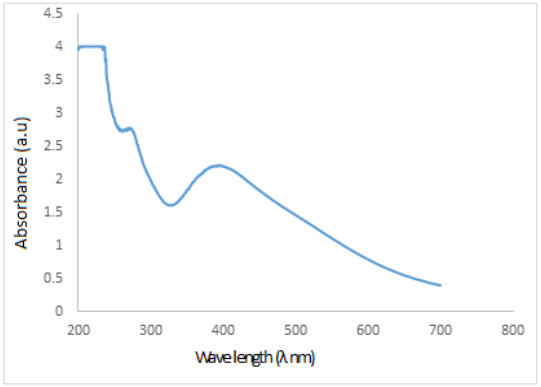


**Figure 2**. UV-vis spectrum of AgNPs

### 3.4.2 High Resolution TEM/SEM

The TEM AND SEM images of the as–produced AgNPs are shown in Figure 3. The TEM image shows spherical shaped, mono-dispersed AgNPs, while the SEM image shows spherical shaped and agglomerated AgNPs.

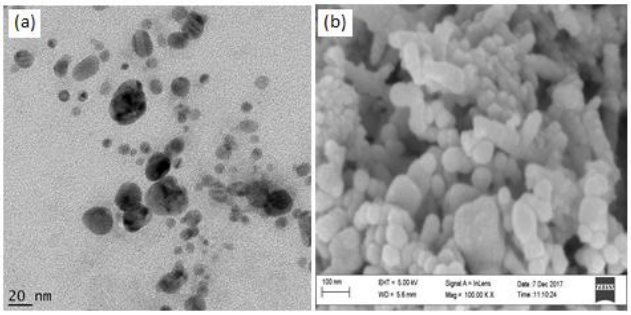


**Figure 3**. (a)TEM image of AgNPs (b) SEM image of AgNPs

### 3.4.3 X-ray Diffraction (XRD)

The XRD pattern of the as-produced AgNPs is shown in Figure 4. All reflections correspond to the presence of silver metal with face-centered cubic symmetry. The diffraction intensities were recorded from $2\theta = 20^{o}$ to $100^{o}$. Five prominent diffraction peaks at $38.2^{o}$, $44.5^{o}$, $64.7^{o}$, $77.5^{o}$ and $81.8^{o}$ shown are in accordance with the JCPDS file corresponds to the set of reflection planes indexed as (111), (200), (220), (311), and (222) respectively. This is similar to published report on XRD of AgNPs [5].

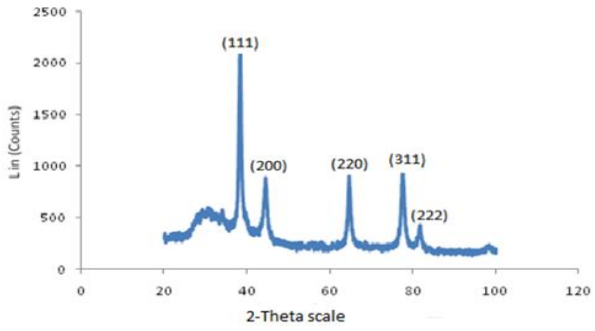


**Figure 4**. XRD pattern of AgNPs

### 3.4.4 Energy Dispersive Spectrum (EDS)

Figure 5 shows the EDS spectrum of as-synthesized AgNPs, with the prominence of silver metal and occurrence of impurities like C, O, Na, Pt, and Pb which are from the plant extract.

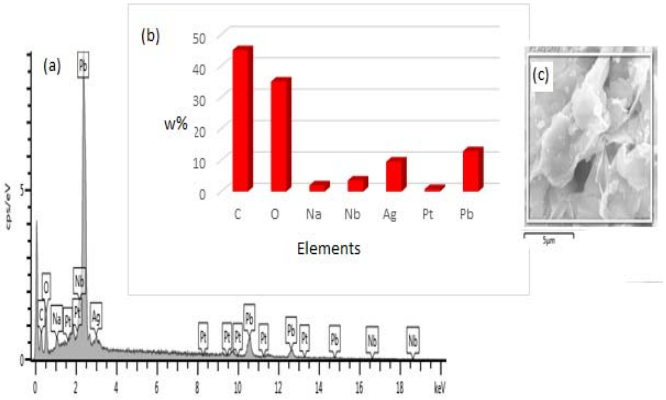


**Figure 5**. EDS spectrum of as-synthesized AgNPs

## 3.5 Influence of Synthesis Parameters on the Crystallite Size of Silver Nanoparticles (AgNPs)

In order to investigate the effect of synthesis parameters on the crystallite size of AgNPs, the interaction between the synthesis factors were plotted on 3D surface plots as shown in Figures 6A-C. It was observed that at higher volume of extract, the crystal size of AgNPs is large. This was caused by slowed reduction reaction of $Ag^{+}$ to $Ag^{0}$ [2]. Oluwaniyi [3] pointed out that the absorption peaks of AgNPs were broader and irregular at higher volume of extract indicating a slow reduction rate of Ag+ to $Ag^{0}$ and existence of AgNPs accompanied by increased size distribution.

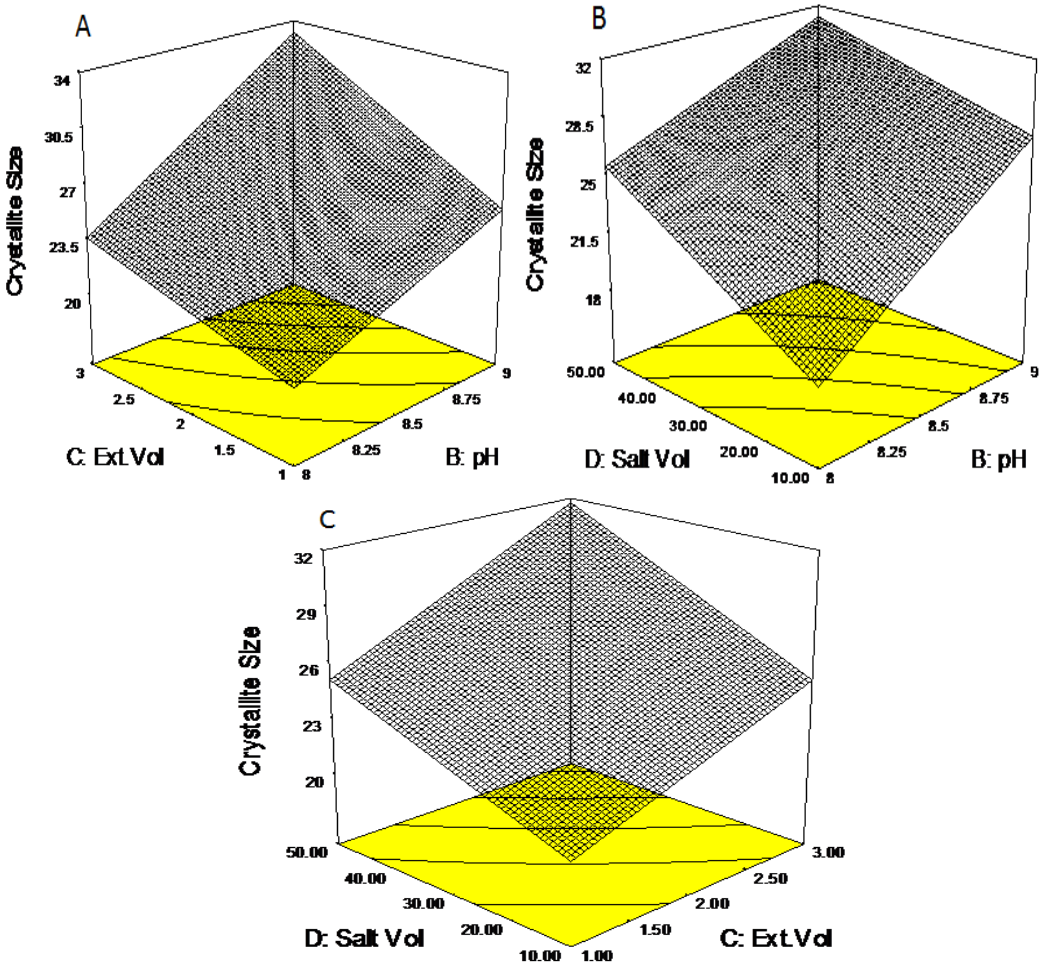


**Figure 6**. (A) Interaction between pH and extract volume; (B) interaction between pH and salt volume; (C) interaction between extract volume and salt volume

It was also observed that as the volume of $Ag^{+}$ solution was increased with respect to the volume of extract, the crystallite size of AgNPs become smaller. This is attributed to existence of more positively charged ions which increased the rate of reaction and hence encouraged the reduction in mean diameter of the NPs. It was reported that as the volume of $Ag^{+}$ solution is increased, the absorption peak becomes sharper with excellent enhancement in the absorption band intensity.

As pH of the reaction mixture is increased from lower values to higher values the mean crystal size of AgNPs becomes smaller. However, an increment in reaction temperature was accompanied by increased growth of crystal size of the nanoparticles. This is attributed to the increase movement of free electrons that resulted to rise in the reaction rate. This is in agreement with the opinion of other researchers [6]. However, it has been reported that increment in reaction temperature above 60 $^{o}$C usually leads to increase in the intensity of SPR band [7] as a result of bathochromic shift which results in a decrease in the mean diameter of AgNPs. This study has shown the practicability of using RSM to optimize the biosynthesis of AgNPs as earlier established by some authors [8-10]

## 4 Conclusion

The optimized synthesis parameters of temperature 35$^{o}$C, pH 8, extract to $AgNO_3$ solution volume ratio of 1:10 produced an optimum crystallite size of 15.4 nm. The characterization of the produced AgNPs showed similar spherical-shaped AgNPs as reported by other researchers. The ANOVA analysis shows that the model as well as the model terms were significant based on P-value <0.05. This means that all the synthesis parameters played a vital role in determining the crystallite size of the synthesized AgNPs.

## Acknowledgements

The authors wish to acknowledge the contribution of Nanotechnology Research Group, Centre for Genetic Engineering and Biotechnology, Federal University Technology, Minna, Niger State, Nigeria, Nanotechnology Research Group (*NANO*$^{+}$), Ladoke Akintola University of Technology, Ogbomoso, Oyo State, Nigeria and all those that contributed technically in this paper.

## References

[1] Rao YS, Kotakadi VS, Prasad TN, Reddy AV and Gopal DS 2013 Green synthesis and spectral characterization of silver nanoparticles from Lakshmi tulasi (*Ocimum sanctum*) leaf extract. *Spectrochim. Acta Part A: Mol. Biomol. Spectr.* **103** pp 156-159.

[2] Singleton, V.L., Orthofer, R. and Lamuela-Raventós, R.M 1999 Analysis of total phenols and other oxidation substrates and antioxidants by means of folin-ciocalteu reagent. *Methods Enzymol.* **299** pp. 152-178.

[3] Oluwaniyi OO, Adegoke HI, Adesuji ET, Alabi AB, Bodede SO, Labulo AH and Oseghale CO 2016 Biosynthesis of silver nanoparticles using aqueous leaf extract of *Thevetia peruviana* Juss and its antimicrobial activities. *Appl Nanosci*. **6** (6) pp 903-912.

[4] Lateef A, Folarin BI, Oladejo SM, Akinola PO, Beukes LS, and Gueguim-Kana EB 2018 Characterization, antimicrobial, antioxidant and anticoagulant activities of silver nanoparticles synthesized from *Petiveria alliacea* L. leaf extract. *Prep. Biochem. Biotechnol.* **48** (7) pp 646-652.

[5] Lateef A, Adelere IA, Gueguim-Kana EB, Asafa TB and Beukes LS 2015 Green synthesis of silver nanoparticles using keratinase obtained from a strain of *Bacillus safensis* LAU 13. *Int. Nano Lett.* **5** (1) pp 29-35.

[6] Ahmed S, Saifullah, Ahmad M, Swami BL and Ikram S 2016 Green synthesis of silver nanoparticles using *Azadirachta indica* aqueous leaf extract. *J. Rad. Res. Appl. Sci*. **9** (1) pp 1-7.

[7] Ibrahim HM 2015 Green synthesis and characterization of silver nanoparticles using banana peel extract and their antimicrobial activity against representative microorganisms. *J. Rad. Res. Appl. Sci.* **8** (3) pp 265-275.

[8] Nyakundi EO and Padmanabhan MN 2015 Green chemistry focus on optimization of silver nanoparticles using response surface methodology (RSM) and mosquitocidal activity: *Anopheles stephensi* (Diptera: Culicidae). *Spectrochim. Acta Part A: Mol. Biomol. Spectr*. **149** pp 978-84.

[9] Yıldız N, Ateş Ç, Yılmaz M, Demir D, Yıldız A and Çalımlı A 2014 Investigation of lichen based green synthesis of silver nanoparticles with response surface methodology. *Green Process. Synth*. **3** (4) pp 259-270.

[10] San Chan Y and Don MM 2013 Optimization of process variables for the synthesis of silver nanoparticles by *Pycnoporus sanguineus* using statistical experimental design. *J. Korean Soc. Appl. Biol. Chem*. **56** (1) pp 11-20.